The Meteoritical Society

Meteoritics & Planetary Science 50, Nr 2, 229–242 (2015)
doi: 10.1111/maps.12414

Fe and O isotope composition of meteorite fusion crusts: Possible natural analogues to chondrule formation?

Dominik C. HEZEL[1,2*], Graeme M. POOLE[1], Jack HOYES[1], Barry J. COLES[3], Catherine UNSWORTH[1], Nina ALBRECHT[4], Caroline SMITH[1], Mark REHKÄMPER[3], Andreas PACK[4], Matthew GENGE[3], and Sara S. RUSSELL[1]

[1]Department of Mineralogy, Natural History Museum, Cromwell Road, SW7 5BD London, UK
[2] Present address: Department of Geology and Mineralogy, University of Cologne, Zülpicher Str. 49b, 50674 Köln, Germany
[3]Department of Earth Science and Engineering, Imperial College, London SW7 2AZ, UK
[4]Geowissenschaftliches Zentrum, Universität Göttingen, Goldschmidtstraße 1, 37077 Göttingen, Germany
[*]Corresponding author. E-mail: dominik.hezel@uni-koeln.de

(Received 18 March 2014; revision accepted 13 November 2014)

Abstract–Meteorite fusion crust formation is a brief event in a high-temperature (2000–12,000 K) and high-pressure (2–5 MPa) regime. We studied fusion crusts and bulk samples of 10 ordinary chondrite falls and 10 ordinary chondrite finds. The fusion crusts show a typical layering and most contain vesicles. All fusion crusts are enriched in heavy Fe isotopes, with δ^{56}Fe values up to +0.35‰ relative to the solar system mean. On average, the δ^{56}Fe of fusion crusts from finds is +0.23‰, which is 0.08‰ higher than the average from falls (+0.15‰). Higher δ^{56}Fe in fusion crusts of finds correlate with bulk chondrite enrichments in mobile elements such as Ba and Sr. The δ^{56}Fe signature of meteorite fusion crusts was produced by two processes (1) evaporation during atmospheric entry and (2) terrestrial weathering. Fusion crusts have either the same or higher δ^{18}O (0.9–1.5‰) than their host chondrites, and the same is true for Δ^{17}O. The differences in bulk chondrite and fusion crust oxygen isotope composition are explained by exchange of oxygen between the molten surface of the meteorites with the atmosphere and weathering. Meteorite fusion crust formation is qualitatively similar to conditions of chondrule formation. Therefore, fusion crusts may, at least to some extent, serve as a natural analogue to chondrule formation processes. Meteorite fusion crust and chondrules exhibit a similar extent of Fe isotope fractionation, supporting the idea that the Fe isotope signature of chondrules was established in a high-pressure environment that prevented large isotope fractionations. The exchange of O between a chondrule melt and an ^{16}O-poor nebula as the cause for the observed nonmass dependent O isotope compositions in chondrules is supported by the same process, although to a much lower extent, in meteorite fusion crusts.

INTRODUCTION

Meteors hit Earth's atmosphere at cosmic speeds of tens of km s^{-1} and, if large enough, produce fireballs and reach Earth's surface. During atmospheric entry, their initial velocity of 12–70 km s^{-1} is decelerated to a terminal velocity of around 3 km s^{-1} and during this the friction of the meteorite in air heats their surface to temperatures of 2000–12,000 K. This melts and ablates the outermost layer of the meteorite for about 5–40 s. Depending on size, an ordinary chondrite loses 75–90% of its initial mass and a carbonaceous chondrite even more. The dynamic pressure in front of the meteor is around 2–5 MPa (Shrbeny, personal communication). The vestige of this violent process is an up to millimeter thin, black fusion crust of solidified melt.

Few Fe isotope data for fusion crusts have been reported, as isotope studies usually focus on bulk chondrites or individual chondrules (e.g., Zhu et al. 2001; Mullane et al. 2005; Needham et al. 2009; Hezel et al. 2010; Wang et al. 2013). Clayton et al. (1986) reported O isotope ratios of fusion crusts. Iron

meteorite fusion crusts have a uniform $\delta^{18}O$ between +14 and +16‰. The fusion crusts of stony meteorites are about 1–3‰ enriched in ^{18}O relative to the interior. Additional Si and K isotope data are reported for fusion crusts (Molini-Velsko et al. 1986; Humayun and Clayton 1995), which show minor differences in stable isotope ratios relative to the bulk meteorite.

Stable isotope studies show that cosmic spherules—sub-mm sized glassy micro-meteorites that were completely molten during atmospheric entry—are enriched in ^{56}Fe, in some cases by up to several tens of per mil relative to the solar system average (Alexander et al. 2002; Engrand et al. 2005; Taylor et al. 2005). They are also enriched in ^{18}O compared to the known meteorite groups (Clayton et al. 1986; Engrand et al. 2005). It is not clear whether the high $\delta^{18}O$ enrichment is due to evaporation (Engrand et al. 2005) or due to exchange with an ^{18}O-enriched upper atmospheric reservoir. No oxygen isotope measurements have yet been conducted at altitudes >70 km.

Chondrules formed during brief high-temperature events (>2000 K) at pressures of 1 to 10 Pa. Bulk chondrules have $\delta^{56}Fe$ values between −1.33‰ and +0.65‰ (Mullane et al. 2005; Needham et al. 2009; Hezel et al. 2010) that were established in evaporation and recondensation processes during chondrule formation in the solar nebula (Hezel et al. 2010). Assuming a closed system, it has been demonstrated by Hezel and Palme (2007) that variable chondrule precursor material cannot be the source of bulk chondrule elemental and isotopic variations. The comparatively small extent of Fe isotope compositions is puzzling, as evaporation in the low-pressure regime of the solar nebula should facilitate Rayleigh distillation and produce isotope variations in the tens of per mil range. However, it has been suggested that chondrule formation occurred at an elevated ambient pressure that suppressed large isotope fractionation (Cuzzi and Alexander 2006; Alexander et al. 2008). A major obstacle to understanding chondrule formation is the lack of any natural analogue material. As the formation of fusion crusts and chondrules involve, in part, similar processes and conditions, such as a brief high-T event and elevated pressures, meteorite fusion crusts might currently be the closest natural analogue to chondrule formation. Comparing findings from Fe isotope signatures of meteorite fusion crusts with chondrule Fe isotope composition might therefore help to elucidate why chondrules only feature a limited range of Fe isotope compositions.

Chondrules from the CV3 chondrite Allende fall on a trend with a slope of ~1 in a $\delta^{17}O$ versus $\delta^{18}O$ diagram (Clayton et al. 1983; Rudraswami et al. 2011). The current explanation for this is an exchange between an initially ^{16}O-rich melt and ^{16}O-poor gas (e.g., Pack et al. 2004; Krot et al. 2006; Chaussidon et al. 2008; Schrader et al. 2013, 2014). Exchange between melt and gas might also occur when the molten outside of a meteorite exchanges elements with the atmosphere during atmospheric entry. The O isotope composition of the atmosphere is well known (Barkan and Luz 2011), and significantly different from chondrite in both $\delta^{18}O$ and $\Delta^{17}O$. An elemental exchange between molten meteorite surface and atmosphere might therefore produce a fusion crust with an intermediate O isotope composition that plots on a nonmass dependent isotope fractionation line between the meteorite and the atmospheric O isotope composition (cf. Clayton et al. 1986).

The first detailed descriptions of fusion crusts are found in Chladni (1819), while Ramdohr (1967, and references therein) provides an excellent summary of optical microscopy studies for a large number of meteorite fusion crust samples. The petrography and petrology of meteorite fusion crusts was further investigated in detail by Genge and Grady (1999).

Here, we present the first systematic study of Fe and O isotope signatures and chemical compositions for bulk meteorites and their associated fusion crusts. We discuss processes during meteorite fusion crust formation and then draw some conclusions regarding chondrule formation conditions.

TECHNIQUES

Sample Selection

We selected about equal numbers of H, L, and LL ordinary chondrites from 10 finds and 10 falls, spanning the entire range of petrologic types (Table 1). The terrestrial ages of most finds are unknown, but these meteorites were presumably exposed to the atmosphere and weathering for up to thousands of years (Jull 2006). From the falls, we selected those samples which exhibited the most pristine fusion crusts. Criteria were (1) short duration of the time interval between fall and recovery of the meteorite; (2) macroscopically unaltered fusion crust, whereby a black and shiny appearance was preferred; and (3) large samples, as fusion crust not in direct contact or proximity to soil will presumably be less affected by weathering.

Sample Preparation and Mass Spectrometry

Approximately 1 g of sample was cut from each meteorite, from which the fusion crust (between 1 and 10 mg for each sample) was removed with a ceramic scalpel. Using a binocular microscope, any fusion crust

Table 1. Meteorite bulk chemical compositions.

	wt%											μg g^{-1}	
Name	Al	Ca	Fe	K	Mg	Na	Cr	Mn	Ni	P	S	Ba	Sr
Falls													
Thal	1.24	1.12	29.22	0.08	15.50	0.64	0.25	0.20	1.51	0.08	1.74	2.4	7.0
Richardton	1.06	1.00	29.30	0.07	13.50	0.52	0.23	0.19	1.93	0.09	1.40	2.0	6.3
Thuathe	1.26	1.18	20.49	0.09	15.80	0.65	0.26	0.22	1.09	0.11	2.15	2.8	7.9
Barwell	1.13	1.16	24.79	0.08	14.77	0.62	0.26	0.22	1.66	0.08	1.92	2.7	7.2
Umm Ruaba	1.17	1.19	22.41	0.09	15.44	0.66	0.21	0.22	1.17	0.07	1.71	2.4	7.2
Nikolskoe	1.16	1.09	25.52	0.08	14.96	0.65	0.25	0.21	1.53	0.07	2.07	2.3	7.1
Dhurmsala	1.39	1.19	20.96	0.09	16.40	0.72	0.25	0.23	0.83	0.08	2.05	2.9	8.8
Bawku	1.30	1.24	18.74	0.09	16.16	0.74	0.26	0.24	0.85	0.09	1.55	2.8	8.4
Finds													
Ovid	1.24	0.96	25.77	0.11	13.45	0.52	0.24	0.18	1.16	0.10	1.14	558.2	24.9
Saline	1.07	0.99	28.59	0.07	13.33	0.49	0.23	0.18	1.60	0.09	1.58	2.7	6.7
Ransom	1.13	1.04	25.00	0.09	13.87	0.46	0.25	0.20	1.27	0.09	1.61	29.8	9.1
Abernathy	1.41	1.16	19.80	0.12	15.44	0.62	0.26	0.23	0.28	0.10	0.61	146.1	24.4
Farnum	1.36	1.04	21.47	0.11	14.17	0.68	0.25	0.23	0.70	0.09	1.45	77.2	12.0
Hardwick	1.22	1.06	20.42	0.08	15.26	0.55	0.23	0.22	0.99	0.09	1.73	2.8	6.3
Oberlin	1.31	1.24	17.70	0.09	16.46	0.68	0.26	0.24	0.81	0.07	0.96	18.7	9.9

pieces with adhering, lightly colored, meteorite materials were excluded from isotope analyses.

The fusion crusts were then powdered in an agate mortar with the addition of 100 μL acetone (Normapur, Fe <0.05 ppm). About 1–2 mg of sample material was dissolved in closed Savillex teflon beakers for at least 24 h at 130 °C in a mixture of 2 mL concentrated HF and 1 mL concentrated HNO_3. The solutions were dried and the residues redissolved in 5 mL HCl for at least 24 h at 130 °C. This second step was repeated. No residual solids, such as undissolved chromite, were found at this stage. The remaining meteorite sample of ~1 g was also powdered in an agate mortar for bulk analysis, and a ~10 mg aliquot was digested with the same procedure used for the fusion crusts (Figs. 1 and 2).

Chromatographic separation of Fe was performed following published methods (Dauphas et al. 2004) using AG1-X8 anion exchange resin, and analyses confirmed that complete recovery of Fe was achieved with this technique. The procedural Fe blank of <50 ng produced a sample to blank ratio of at least 5000:1, thereby introducing only a negligible error.

The Fe isotope compositions were measured at the MAGIC Laboratories of Imperial College London, using a Nu Plasma HR instrument in conjunction with a Nu Instruments DSN desolvating nebuliser for sample introduction. The analyses were carried out in pseudo high-resolution mode, with a 0.03 mm source slit. This configuration provided a mass resolving power of ~7500 and sufficient transmission to allow routine analyses of 2 ppm Fe sample solutions. The external reproducibility of the data was typically ±0.07‰ (2SD) for δ^{56}Fe and ±0.15‰ (2SD) for δ^{57}Fe, while the internal (within-run) reproducibility (2SE) was generally about a factor of two better. All samples measured were analyzed between three and six times, nonconsecutively, during analytical sessions of about 8 h duration. Each sample measurement was bracketed by at least two analyses of an IRMM-014 Fe solution that was made up to closely match the Fe concentration of the sample. The average results obtained from these multiple analyses are reported here, using the δ-notation relative to the IRMM-014 Fe standard.

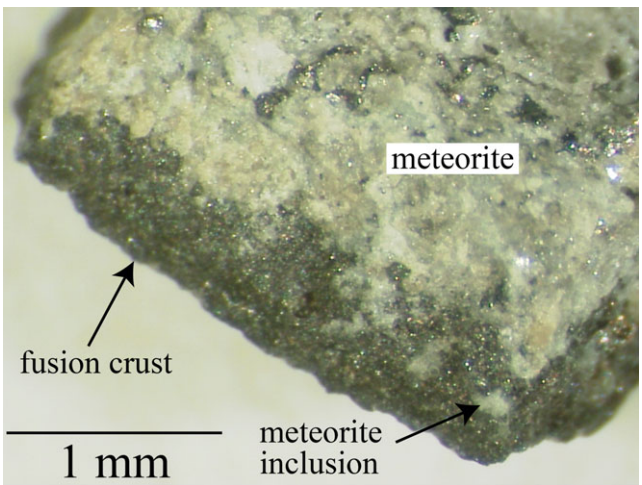

Fig. 1. Optical photomicrograph of the Umm Ruaba L5 fall. A small bit of meteorite inclusion in the fusion crust is indicated by an arrow.

Oxygen isotope ratios were analyzed by laser-assisted fluorination (Sharp 1990) following analytical protocols that were previously described in detail (Pack

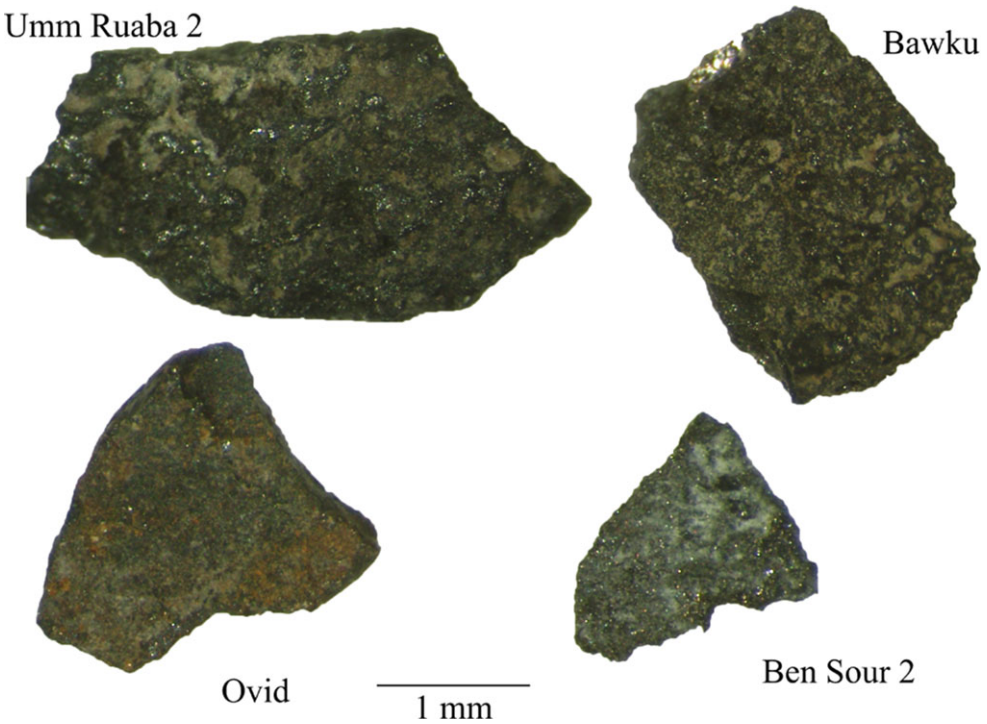

Fig. 2. Optical photomicrographs of four meteorite fusion crusts that were carefully separated with a ceramic scalpel under a binocular microscope.

et al. 2013). In brief, samples were heated with a 50 W infrared laser in an atmosphere of ~20 mbar purified F_2 gas. The liberated O_2 was passed through a gas chromatograph before being introduced into the source of a MAT 253 gas mass spectrometer. The gas was analyzed in continuous flow mode. Accuracy and precision (2SD) were ~0.2‰ for $\delta^{18}O$, ~0.1‰ for $\delta^{17}O$, and ~0.05‰ for $\Delta^{17}O$. The $\Delta^{17}O$ values are reported using the linearized form of the δ notation (Miller 2002) relative to a line defined by rocks and minerals with a slope of $\lambda = 0.5251$. We use the $\Delta^{17}O$ of MORB to ensure that $\delta^{17}O$ is reported on the VSMOW scale (Pack and Herwartz 2014). The uncertainty in $\Delta^{17}O$ is smaller than expected from Gaussian error propagation of $\delta^{17}O$ and $\delta^{18}O$ because of the high degree of correlation between the errors in $\delta^{17}O$ and $\delta^{18}O$.

Electron Microprobe Analyses

Chemical analyses of the silicate phases were obtained by means of the CAMECA SX100 electron microprobe at the Natural History Museum, London, equipped with five wavelength dispersive spectrometers. The accelerating voltage was set to 20 kV, the beam current to 20 nA, and the spot size to 1 μm. The following standards have been used; detection limits in wt.%. Si, synthetic fayalite: 0.02; Ti, synthetic rutile: 0.04; Al, synthetic corundum: 0.02; Cr, synthetic chromium oxide: 0.04; Fe synthetic fayalite: 0.04; Mn synthetic MnTiO3: 0.06; Ni synthetic NiO: 0.06; Mg synthetic forsterite: 0.02; Ca, natural wollastonite: 0.03; Na, jadeite: 0.04. The built in PAP-algorithm (e.g., Pouchou and Pichoir 1991) was used for correction.

Bulk Meteorite Analyses

Bulk concentrations of major and minor elements were measured by means of ICP-AES (Varian Vista Pro-Axial) at the Natural History Museum, London (NHM). For this, 40 mg of sample, pretreated with 1 mL concentrated HNO_3, were fused with 120 mg of $LiBO_2$ in a Pt/Au crucible and the resulting flux dissolved in 10% HNO_3. Bulk concentrations of trace elements were measured by means of quadrupole ICP-MS (Varian), also at the NHM. For this, 100 mg of sample were pretreated with concentrated HNO_3 and then dissolved in a mixture of 4 mL HF and 1 mL $HClO_4$ at 100 °C. This solution was dried at 150 °C and the residue redissolved at 150 °C using 2 mL $HClO_4$. The solution was dried again, re-dissolved in a mixture of 1 mL concentrated HNO_3 + 1 mL H_2O + 0.5 mL H_2O_2 at 70 °C, and then made up to 10 mL with water. Nonisobaric interferences during the ICP-MS analyses were reduced by tuning CeO/Ce^+ to <1%

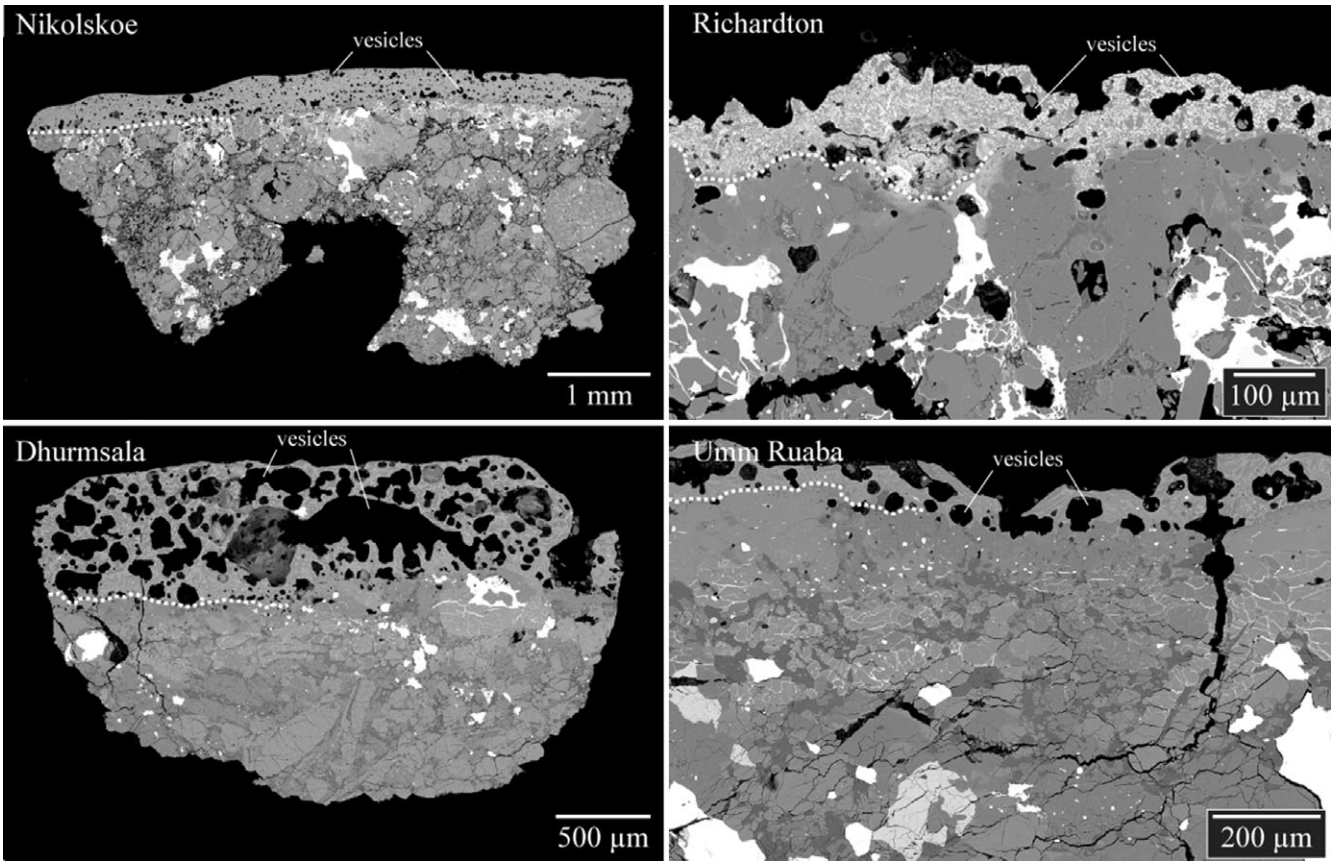

Fig. 3. Backscatter electron images of four meteorites and their fusion crusts. The border of the melt layer to the interior of the meteorite is partly indicated by a dotted line on the left of each sample.

and Ba^{2+}/Ba^{+} to <1%. For Eu, Gd, Tb, Hf, and W, the levels of polyatomic interferences were estimated using single-element standards and the calculated concentration data were corrected accordingly. Concentrations of Ga (using ^{71}Ga) were corrected for $^{142}REE^{++}$. The certified reference materials BCR-1, BHVO-1 (basalts), JG-1 (granodiorite), JLS-1 (limestone), and MAG-1 (marine mud) were analyzed repeatedly to monitor the accuracy of the elemental analyses.

RESULTS

Petrography and Petrology

The studied fusion crusts comprise two distinct layers: an outer melted fusion crust containing quench crystals, relict grains and glass, and an inner substrate that shows evidence for partial melting of selected phases. The melted outer fusion crusts vary in thickness from tens of µm to ~1 mm (Fig. 3) and nearly all contain vesicles. The substrate below forms a layer up to 500 µm in thickness and is texturally distinct from the underlying meteorite. The boundary between the outer melted crust and the thermally altered substrate is marked by the appearance of quench crystals in the melted crust.

The melted outer crust on the samples is comprised largely of olivine quench crystals with interstitial aluminosilicate glass containing micron-sized, often dendritic, iron oxides. Quench crystals are elongate dendrites in Richardton, Umm Ruaba, and Dhurmsala. Pyroxene, feldspar, chromite, and ilmenite also occur in the fusion crust and are probably relict unmelted grains. Ramdohr (1967) reports magnetite as a common mineral in fusion crusts, which we cannot confirm, as individual grains are often too small for accurate quantitative analyses. Qualitative SEM analyses indicate the occurrence of various oxides, probably spinel, containing Mg, Al, Ti, Cr, and Fe, but none of the grains only contains Fe, probably due to matrix overlap with surrounding phases. The molten crust is usually metal free. Vesicles within the molten crust vary from small subspherical cavities to large irregular voids up to 500 µm in size. Mineral compositions are shown in Table 2.

The thermally altered substrate comprises two distinct layers. An upper metal-poor layer, 100–200 μm in width, has glassy chondrule mesostasis containing feldspars with diffuse boundaries with the surrounding melt, and rounded metal and sulfide grains. In places (e.g., Richardton; Fig. 3), short veins of the molten crust extend into this layer. Veins comprise quench olivine and glass, but lack iron oxide dendrites. The lower layer of the thermally altered substrate contains abundant, interlinked metal-sulfide veins up to 10 μm in diameter.

The bulk chondrite elemental compositions of the studied falls are almost unfractionated relative to H chondrites (Table 1, Fig. 4). In contrast, the bulk chondrite elemental compositions of most of the studied finds have variable enrichments in the mobile alkali elements Ba (up to 100× H chondrite) and Sr (up to 3× H chondrite).

Fe Isotope Compositions

The bulk Fe isotope composition of chondrite finds and falls are, within uncertainty, identical to the IRMM-014 standard (Table 3; Fig. 5) and in agreement with previous literature values (Needham et al. 2009; Craddock and Dauphas 2011).

The fusion crusts show a ubiquitous enrichment in heavy Fe isotopes, with fractionations of up to +0.35‰ for δ^{56}Fe (Fig. 5). The mean δ^{56}Fe value of fusion crusts from finds is +0.23‰, which is 0.08‰ higher than the mean δ^{56}Fe of fusion crusts from falls, which is +0.15‰. While the mean δ^{56}Fe values determined for the falls and finds just overlap with the 2se uncertainties, they are distinct when the medians are considered, which are more appropriate due to the irregular distribution of the data points. While fusion crusts with low Sr and Ba concentrations have variable δ^{56}Fe, all fusion crusts enriched in Sr and Ba have high δ^{56}Fe values (Fig. 6). Further, there seems to be an upper limit of δ^{56}Fe values, with a maximum Fe isotope fractionation of about +0.4‰. There are no correlations between δ^{56}Fe and class or petrologic type of meteorite.

O Isotope Compositions

We analyzed aliquots of eight bulk chondrite and five fusion crust samples from falls as well as seven bulk chondrite and three fusion crust samples from finds (Table 4). Bulk chondrites and their corresponding fusion crusts have slightly different O-isotopic compositions. In five of the eight studied meteorites, the fusion crusts have δ^{18}O values that are 0.9–1.5‰ higher compared to the respective bulk chondrite. The three meteorites Umm Ruaba, Bawku, and Thuathe have the same δ^{18}O within uncertainty (Fig. 7).

DISCUSSION

Petrography and Petrology

The petrology and mineralogy of the fusion crusts testify to progressive melting and oxidation from the interior of the meteorite to the outer crust. The innermost layer of the thermally altered substrate is dominated by metal-sulfide veins representing eutectic Fe-Ni-S melts generated at 994 °C. Differential thermal stress may be responsible for the generation of the vein networks into which this melt injected. They are clearly the result of entry heating since they are absent within the underlying meteorite. Migration of metal-sulfide liquids within this layer may be an important process for the redistribution of siderophile elements.

The outer layer of the thermally altered substrates contain textural evidence for partial melting of the aluminosilicate glass mesostasis of chondrules as previously described by Genge and Grady (1999). Subspherical vesicles are present within the mesostasis indicating these were capable of flow. Vesicles are exceedingly rare within chondrules and are probably generated in fusion crust by oxidation of reduced volatiles within the glass (Genge and Grady 1999). Diffuse boundaries on feldspars are present in mesostasis, suggesting partial melting of these phases. Except for large (>100 μm) grains, most metal and sulfide within this layer occurs as small droplets (<20 μm in size), which are probably immiscible Fe-S eutectic liquids.

The outer fusion crusts have a quench texture of elongate olivine phenocrysts within a mesostasis containing glass and dendritic iron oxide. This texture is typical of crystallization during rapid cooling and would have formed by cooling of fusion crust after the end of luminous flight. Larger olivine and pyroxene grains in some fusion crusts, however, are rounded and resorbed and thus probably relict unmelted grains liberated from the underlying substrate. Irregular chromite and ilmenite are also probably relicts.

The frequent occurrence of vesicles in fusion crusts runs contrary to the generally low volatile contents of ordinary chondrites. Vesicles may, however, form by oxidation of sulfide melts to SO_2 (Thaisen and Taylor 2009). The high abundance of vesicles in some fusion crust suggests rapid formation of vesicles. This is more compatible with oxidation of sulfide melts rather than bubble growth by exsolution of volatiles from the melt. In places (e.g., Dhurmsala, Fig. 3), cavities extend entirely through the molten fusion crust and expose the thermally altered substrate, perhaps due to rapid degassing. Large composite vesicles may play a role in loss of fusion crust melt by ablation, as they can

Table 2. Electron microprobe analyses of fusion crusts.

	Nikolskoe (L4)		Umm Ruaba (L5)				Barwell(L6)		Dhurmsala (LL6)			Richardton (H5)			Saline(H5)					Thal-H6
	ol	px	ol	px	fsp	chr	ol	px	ol	px	px	ol	ol	px	ol	px	fsp	ilm	ilm	ol
SiO_2	38.41	55.78	39.43	55.65	66.77	0.92	39.08	56.58	38.48	56.09	54.94	40.10	33.11	57.01	34.61	51.48	51.38	0.12	0.08	39.00
TiO_2	<d.l.	0.26	0.10	0.20	0.03	1.98	0.01	0.19	<d.l.	0.24	0.23	0.03	0.11	0.26	0.11	0.91	0.09	53.17	54.09	<d.l.
Al_2O_3	<d.l.	0.20	2.01	0.15	21.44	6.63	<d.l.	0.28	<d.l.	0.25	0.59	<d.l.	2.84	0.42	0.03	2.87	29.52	0.10	0.11	<d.l.
Cr_2O_3	0.01	0.16	0.47	0.12	0.06	56.27	0.02	0.10	0.01	0.14	0.49	0.04	0.32	0.33	0.01	0.71	0.00	0.11	0.16	0.03
FeO	23.40	14.27	28.53	14.01	0.59	28.22	22.82	13.83	24.99	15.08	11.81	16.83	43.74	10.71	41.38	8.62	0.90	41.92	40.57	17.67
MnO	0.49	0.50	0.35	0.51	0.01	0.49	0.48	0.47	0.46	0.46	0.37	0.44	0.27	0.49	0.49	0.20	<d.l.	0.45	0.45	0.49
NiO	0.02	0.04	0.94	0.00	0.01	0.11	<d.l.	0.06	0.02	0.01	0.03	0.02	1.36	<d.l.	<d.l.	0.01	0.01	<d.l.	<d.l.	0.02
MgO	38.73	29.18	26.68	28.66	0.01	2.91	39.38	29.35	37.70	28.56	22.98	44.25	15.06	31.58	23.11	16.47	0.19	3.28	4.04	42.02
CaO	0.01	0.73	1.57	0.88	2.66	0.08	0.02	1.01	0.05	0.76	9.29	<d.l.	1.90	0.84	0.43	18.44	14.06	0.20	0.24	0.01
Na_2O	<d.l.	0.01	0.69	0.01	8.64	0.14	0.01	0.05	<d.l.	0.01	0.29	<d.l.	1.23	0.03	<d.l.	0.21	3.59	<d.l.	<d.l.	<d.l.
K_2O	<d.l.	<d.l.	0.09	<d.l.	0.73	0.03	<d.l.	<d.l.	<d.l.	<d.l.	0.02	<d.l.	0.15	<d.l.	<d.l.	<d.l.	0.09	<d.l.	<d.l.	<d.l.
Total	101.05	101.14	100.86	100.19	100.95	97.78	101.80	101.92	101.70	101.60	101.04	101.71	100.09	101.67	100.17	99.92	99.83	99.34	99.74	99.23
Si	0.994	1.978	1.050	1.989	2.907	0.033	1.000	1.986	0.996	1.985	1.979	0.998	0.978	1.978	0.993	1.905	2.352	0.003	0.002	1.001
Ti	<d.l.	0.007	0.002	0.005	0.001	0.053	0.000	0.005	<d.l.	0.006	0.006	0.001	0.002	0.007	0.002	0.025	0.003	0.991	0.996	<d.l.
Al	<d.l.	0.008	0.063	0.006	1.100	0.279	<d.l.	0.012	<d.l.	0.010	0.025	<d.l.	0.099	0.017	0.001	0.125	1.593	0.003	0.003	<d.l.
Cr	0.000	0.004	0.010	0.003	0.002	1.590	0.000	0.003	0.000	0.004	0.014	0.001	0.007	0.009	0.000	0.021	0.000	0.002	0.003	0.001
Fe	0.506	0.423	0.635	0.419	0.021	0.843	0.488	0.406	0.541	0.446	0.356	0.350	1.080	0.311	0.993	0.267	0.034	0.869	0.831	0.379
Mn	0.011	0.015	0.008	0.015	0.000	0.015	0.010	0.014	0.010	0.014	0.011	0.009	0.007	0.014	0.012	0.006	<d.l.	0.009	0.009	0.011
Ni	0.000	0.001	0.020	0.000	0.000	0.003	<d.l.	0.002	0.000	0.000	0.001	0.000	0.032	<d.l.	<d.l.	0.000	0.000	<d.l.	<d.l.	0.000
Mg	1.494	1.543	1.059	1.527	0.001	0.155	1.502	1.536	1.455	1.507	1.234	1.642	0.663	1.633	0.989	0.909	0.013	0.121	0.147	1.607
Ca	0.000	0.028	0.045	0.034	0.124	0.003	0.001	0.038	0.001	0.029	0.359	<d.l.	0.060	0.031	0.013	0.731	0.690	0.005	0.006	0.000
Na	<d.l.	0.001	0.036	0.001	0.729	0.010	0.000	0.003	<d.l.	0.001	0.020	<d.l.	0.070	0.002	<d.l.	0.015	0.319	<d.l.	<d.l.	<d.l.
K	<d.l.	<d.l.	0.003	<d.l.	0.041	0.001	<d.l.	<d.l.	<d.l.	<d.l.	0.001	<d.l.	0.006	<d.l.	<d.l.	<d.l.	0.005	<d.l.	<d.l.	<d.l.
Total	3.006	4.009	2.931	4.001	4.926	2.985	3.001	4.004	3.004	4.002	4.006	3.001	3.005	4.003	3.004	4.004	5.010	2.003	1.999	2.999

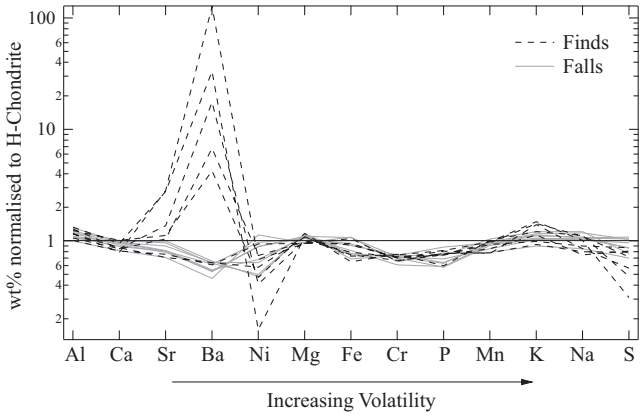

Fig. 4. Bulk chondrite compositions normalized to H chondrite and elements sorted by volatility.

delaminate melt from the underlying substrate. Oxidative degassing, probably of sulfides, therefore, may be crucial in the physical evolution of fusion crust and the ablation rate.

The bulk chemical compositions of all falls are virtually unfractionated relative to average H chondrites (Lodders and Fegley 1998; Fig. 4), while the finds are variably enriched in Ba and Sr and feature some depletion in S. Such fractionations are typical of weathered meteorites, as reported by Al-Kathiri et al. (2005) and Hezel et al. (2011). This indicates that many of the studied finds exchanged material with their surrounding terrestrial environment. In contrast, the falls are unaffected by such exchange, as expected.

Table 3. Fe isotope composition of bulk meteorites and their fusion crusts.

		Bulk					Fusion crust					
Name	Type	n	δ^{56}Fe	2 SE	δ^{57}Fe	2 SE	n	δ^{56}Fe	2 SE	δ^{57}Fe	2 SE	BM number
Falls												
Thal	H6	6	−0.06	0.05	−0.13	0.17	6	0.30	0.03	0.40	0.12	1954,223
		5	0.09	0.07	0.13	0.11						
Richardton	H5	6	0.10	0.12	0.13	0.14	6	0.00	0.03	0.00	0.12	1920,509
		6	−0.04	0.03	−0.08	0.06						
		6	−0.12	0.07	−0.18	0.20						
Thuathe	H4	6	−0.09	0.10	−0.16	0.17	6	0.09	0.03	0.14	0.09	2003,M11
		6	−0.21	0.05	−0.31	0.13						
Barwell	L6	6	0.02	0.06	0.03	0.14	6	0.20	0.05	0.25	0.10	1966,62
		6	−0.05	0.07	−0.05	0.12						
Umm Ruaba	L5	6	0.04	0.09	0.06	0.10	6	0.21	0.10	0.25	0.14	1967,259
		6	−0.06	0.07	−0.05	0.22						
Nikolskoe	L4	6	−0.07	0.07	−0.08	0.09	6	0.04	0.04	0.06	0.10	1956,326
Dhurmsala	LL6	6	0.02	0.06	0.03	0.21	6	0.07	0.07	0.06	0.05	1985,M152
		5	−0.01	0.05	−0.02	0.14						
Bawku	LL5	6	0.08	0.06	0.05	0.15	6	0.14	0.03	0.15	0.07	1995,M2
Witsand Farm	LL4		–	–	–	–	6	0.26	0.06	0.40	0.12	1948,295
Average			*−0.02*	*0.07*	*−0.04*	*0.14*		*0.15*	*0.05*	*0.19*	*0.10*	
Median			*−0.01*	*0.07*	*−0.01*	*0.14*		*0.14*	*0.04*	*0.15*	*0.10*	
Finds												
Ovid	H6	5	0.04	0.07	0.03	0.07	6	0.32	0.04	0.46	0.09	1959,922
Saline	H5	6	−0.09	0.06	−0.09	0.17	6	0.20	0.05	0.25	0.12	86522
Ransom	H4	5	−0.07	0.06	−0.12	0.07	6	0.13	0.03	0.16	0.10	1949,861
Abernathy	L6	4	−0.01	0.05	−0.01	0.08	6	0.20	0.07	0.26	0.14	1959,842
Farnum	L5	6	0.07	0.06	0.10	0.06	6	0.24	0.05	0.26	0.08	1959,861
		6	0.02	0.07	0.08	0.10						
		5	−0.03	0.05	−0.03	0.15						
Hardwick	L4	6	0.03	0.06	0.04	0.08	6	0.05	0.05	0.12	0.14	1959,1035
Mellenbye	LL6		–	–	–	–	6	0.22	0.02	0.21	0.09	1934,623
Oberlin	LL5	6	0.02	0.10	0.06	0.13	6	0.35	0.03	0.42	0.05	1959,779
Ben Sour	LL6		–	–	–	–	6	0.21	0.03	0.31	0.08	2009,M9
UAE 013	L6		–	–	–	–	6	0.34	0.04	0.45	0.13	2009,M12
Average			*−0.01*	*0.07*	*0.00*	*0.10*		*0.23*	*0.04*	*0.29*	*0.10*	
Median			*0.02*	*0.06*	*0.03*	*0.08*		*0.22*	*0.04*	*0.26*	*0.09*	

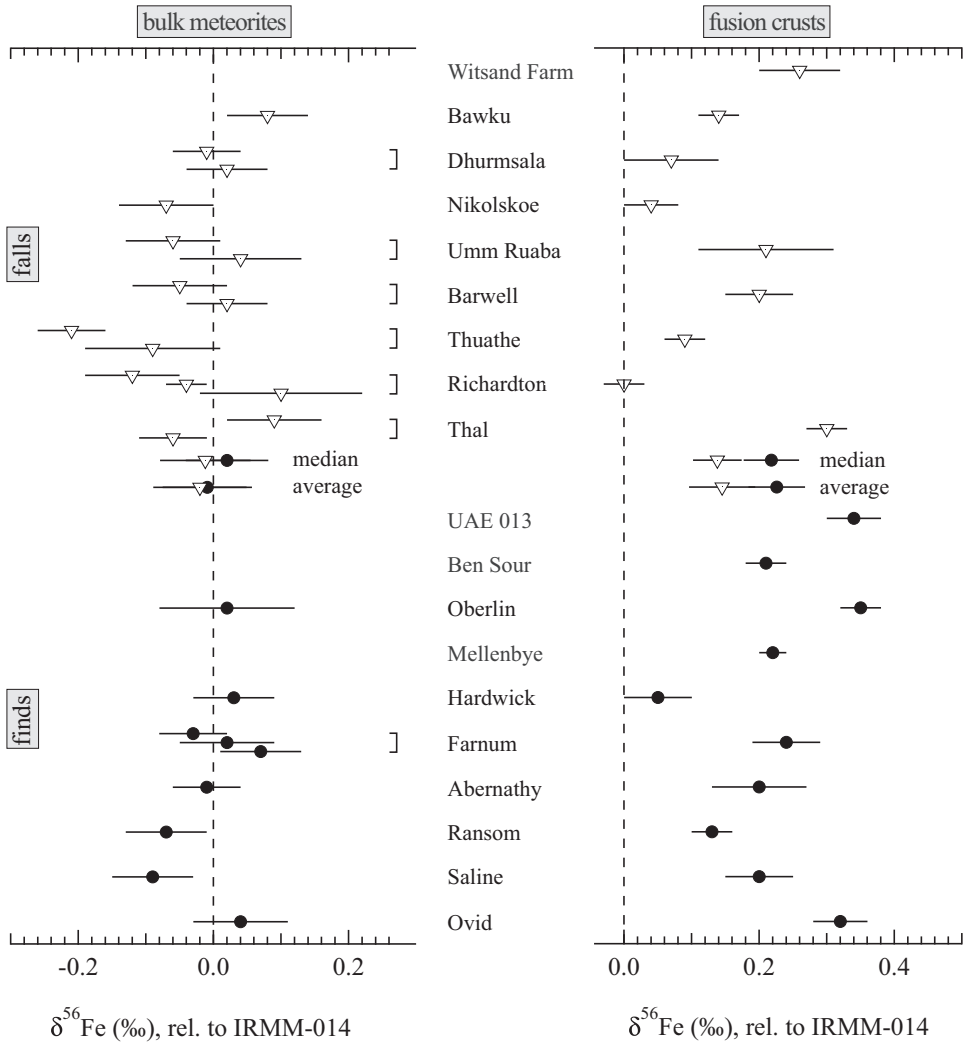

Fig. 5. Fe isotope compositions of bulk chondrites and their fusion crusts. Error bars are 2 SD.

Fe Isotopes

Saunier et al. (2010) demonstrated that meteorites with significant terrestrial weathering are slightly enriched in heavy Fe isotopes with δ^{56}Fe values of up to $+0.071 \pm 0.035‰$. The results of Saunier et al. (2010) and our results (see below), as also suggest that this value represents an upper limit. Therefore, any δ^{56}Fe larger than about $+0.07‰$ is most probably not the result of terrestrial weathering. The fusion crusts of this study have δ^{56}Fe of up to $+0.35‰$, indicating that their Fe isotope composition is the result of fusion crust formation. All fusion crusts display heavy Fe isotope compositions (equivalent to positive δ^{56}Fe), as is expected for the residue of an evaporation process. Pure Rayleigh distillation into vacuum produces Fe isotope fractionations of up to several tens of per mil. Elevated gas pressure above a melt, as present during atmospheric entry, reduces the extent of isotope fractionation because this supports back reaction. We, hence, interpret the heavy Fe isotope compositions of fusion crusts as an evaporative effect in the high-pressure environment that is prevalent during atmospheric entry.

Most meteorite finds reside on Earth for several thousands to ten thousands of years, with occasional terrestrial ages up to 250 ka (Jull 2006). Hence, the fusion crust of δ^{56}Fe of finds might be particularly affected by terrestrial weathering. And, in fact, the average δ^{56}Fe of finds of fusion crusts is $0.08‰$ higher than the average δ^{56}Fe of fusion crusts from falls. This $0.08‰$ difference we find is therefore indistinguishable, within error, from the $+0.07‰$ maximum heavy Fe isotope enrichment determined for terrestrial weathering of meteorites by Saunier et al. (2010). The heavier average Fe isotope composition of find fusion crusts can therefore be explained by terrestrial weathering. The

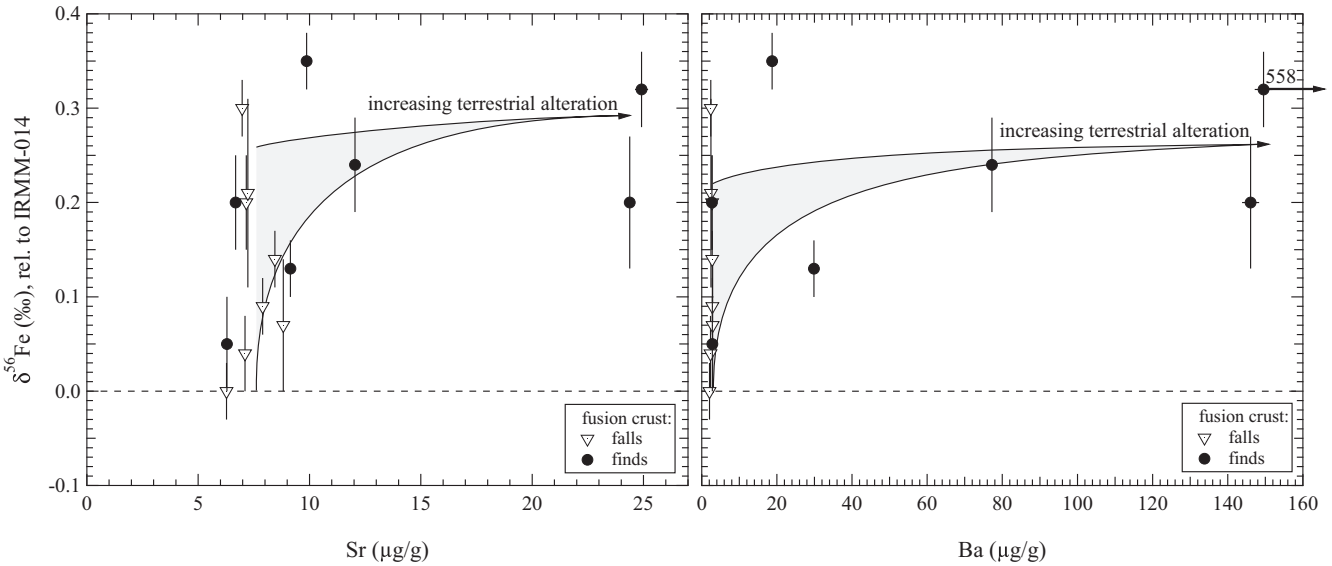

Fig. 6. Fe isotope composition of falls and finds fusion crusts versus bulk chondrite Sr and Ba contents. Chondrites with high Sr and Ba are always high in δ^{56}Fe.

Table 4. O isotope composition of bulk meteorites and their fusion crusts.

		Bulk					Fusion crust					
Name	Type	$\delta'^{18}O$	$\delta'^{17}O$	$\delta^{18}O$	$\delta^{17}O$	$\Delta^{17}O$	$\delta'^{18}O$	$\delta'^{17}O$	$\delta^{18}O$	$\delta^{17}O$	$\Delta^{17}O$	Theta
Falls												
Thal	H6	4.19	2.66	4.20	2.67	0.46	5.01	3.11	5.02	3.12	0.48	0.55
Richardton	H5	5.03	3.05	5.04	3.05	0.41						
Thuathe	H4	5.08	3.26	5.10	3.27	0.59	4.78	3.09	4.79	3.10	0.58	
Barwell	L6	4.80	3.77	4.81	3.78	1.25						
Umm Ruaba	L5	4.70	3.59	4.71	3.60	1.12	4.55	3.63	4.56	3.64	1.24	
Nikolskoe	L4	5.40	3.71	5.41	3.72	0.88	6.85	4.53	6.87	4.54	0.93	0.56
Dhurmsala	LL6	5.45	4.08	5.46	4.08	1.22						
Bawku	LL5	5.55	4.03	5.56	4.04	1.12	5.39	4.04	5.40	4.05	1.21	
Finds												
Ovid	H6	5.98	3.66	5.99	3.66	0.52						
Saline	H5	5.69	3.43	5.71	3.43	0.44	6.64	3.99	6.66	4.00	0.50	0.59
Ransom	H4	5.43	3.43	5.44	3.44	0.58						
Abernathy	L6	5.51	3.98	5.53	3.99	1.08	6.66	4.08	6.68	4.09	0.58	
Hardwick	L4	6.00	4.10	6.02	4.11	0.95						
Oberlin	LL5	5.59	4.20	5.61	4.21	1.26	6.53	3.83	6.55	3.84	0.40	
MORB		5.88	3.03	5.90	3.03	−0.06						
MORB		5.84	3.04	5.86	3.05	−0.03						
MORB		5.42	2.86	5.43	2.86	0.01						
MORB		5.34	2.67	5.35	2.67	−0.13						
MORB		5.73	2.93	5.75	2.93	−0.08						
MORB		5.65	2.84	5.67	2.85	−0.13						

isotopic contribution from weathering to finds is also supported by the observation that such fusion crusts have elevated bulk chondrite Ba and Sr concentrations. As can be seen from Fig. 6, all fusion crusts with high bulk chondrite concentrations of Ba and Sr also have high δ^{56}Fe values, but these level off and stay at a maximum of $\delta^{56}Fe = +0.35 \pm 0.03‰$, even with largely increasing bulk chondrite Ba and Sr abundances. A similar trend for bulk chondrites was found by Saunier et al. (2010) for increasingly weathered meteorites. Subtracting the effects of terrestrial weathering, the highest δ^{56}Fe of fusion crusts in this study is +0.30‰

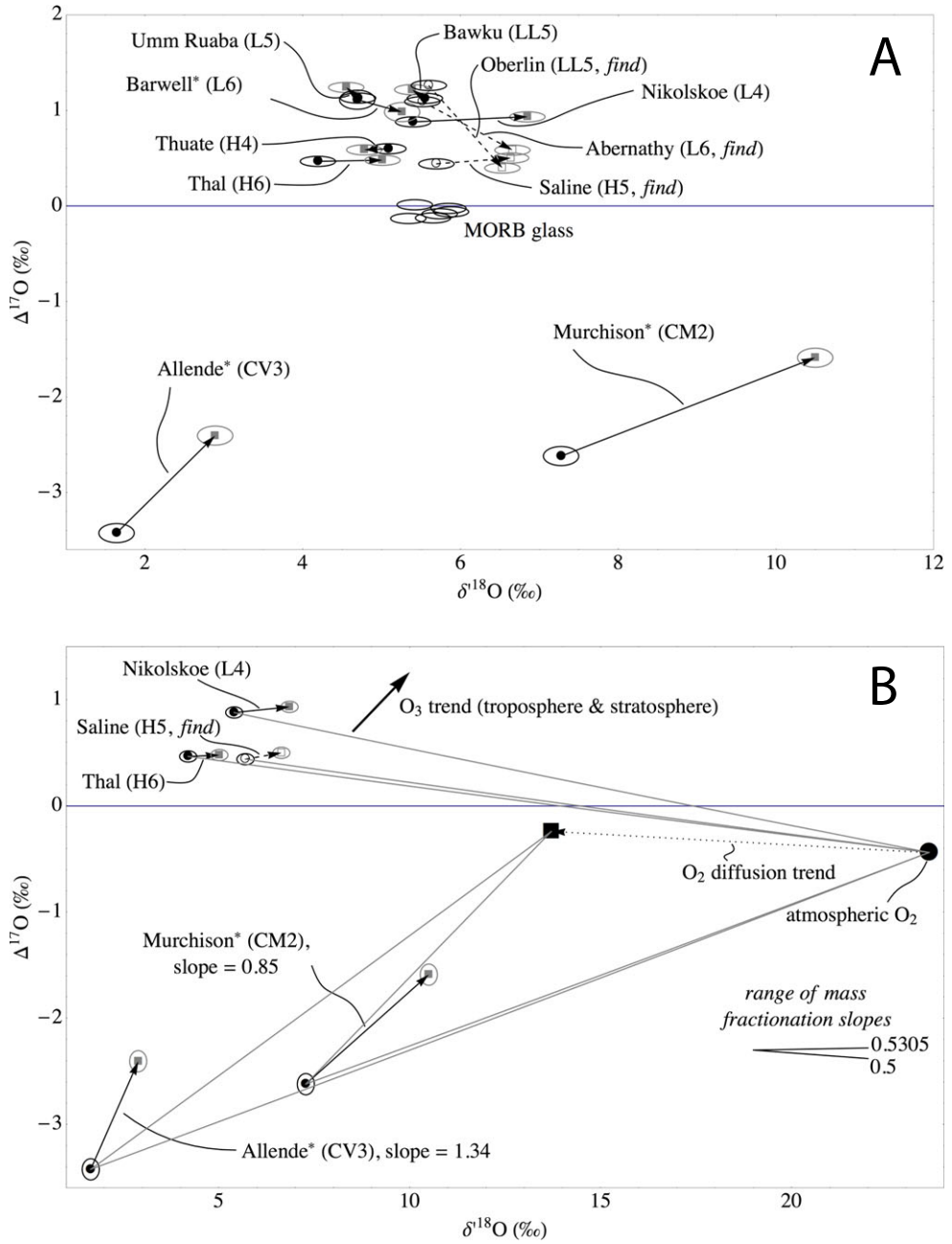

Fig. 7. Bulk chondrite compositions (black symbols) and their fusion crusts (gray symbols). Solid arrows indicate the change in O isotope composition in the fusion crusts due to a combination of processes during atmospheric entry and terrestrial weathering. Dashed lines in the lower plot indicate mixing lines between an unfractionated and a fractionated atmospheric reservoir. The meteorite ellipses represent 2 SD. *Data from Clayton et al. (1986).

for falls (Thal) and +0.27‰ for finds (Oberlin: +0.35‰ minus a maximum terrestrial contribution of 0.08‰).

The find UAE 013 has a terrestrial age of 1.1 ka (Hezel et al. 2011) and a fusion crust with a δ^{56}Fe value of +0.34‰. This is the second highest δ^{56}Fe value determined in this study and, hence, most probably reflects, in part, a terrestrial contribution. If correct, this indicates that a maximum of 1.1 ka are required to increase the Fe isotope composition to the maximum value for terrestrial weathering.

O Isotopes

The fusion crusts of the falls Bawku, Umm Ruaba, and Thuathe are indistinguishable in δ^{18}O and Δ^{17}O within error from the interior of their host meteorites

(Fig. 7A). The fusion crusts of the falls Thal and Nikolskoe as well as the find Saline have a $\delta^{18}O$ that is up to 1.5‰ higher compared to the interior (Fig. 7A). Fusion crust data by Clayton et al. (1986) on the fall Barwell (L6) show a ~1‰ enrichment in ^{18}O for the fusion crust compared to the interior demonstrating that the small fractionation between fusion crust and meteorite interior is likely not due to terrestrial weathering. The data from this study and Clayton et al. (1986) show that only little overall exchange occurs between fusion crust and ambient atmosphere. If equilibrium fractionation between silicate melt and O_2 is negligible at high temperatures, one would expect fusion crusts, which entirely exchanged with O_2, to have $\delta^{18}O$ values identical to atmospheric O_2 at 23.5‰ (Kroopnick and Craig 1972). The observed enrichment of up to 1.5‰ in $\delta^{18}O$ for the fusion crust of ordinary chondrites (this study and Clayton et al. 1986) would be explained by ≤8% exchange with atmospheric O_2. The small degree of exchange is explained by the short time available for equilibration. While fusion crusts are only about a mm thick, the residence time of melt in the fusion layer may only be in the range of seconds before ablation occurs. Although occurring at high total gas pressure, the degree of exchange is therefore much smaller than suggested for chondrules (e.g., Yu et al. 1995; Chaussidon et al. 2008; Schrader et al. 2013, 2014). Chondrules, however, exchanged with H_2O vapor, whereas fusion crust exchanges with air O_2, which is known to be less reactive with respect to O isotope exchange.

If the small observed $\delta^{18}O$ enrichment of fusion crusts is due to mixing of equilibrated (with atmospheric O_2) and unequilibrated (closed system melted meteorite) material, it is expected that the composition of the fusion crusts should fall on binary mixing lines (meteorite, atmospheric O_2) in a $\Delta^{17}O$ versus $\delta^{18}O$ diagram (see Choi et al. 2007). All meteorite fusion crusts, however, fall above such simple mixing trends (Fig. 7B). This is notably the case for the Clayton et al. (1986) data for Allende and Murchison, which also show larger fractionation in $\delta^{18}O$ between bulk meteorite and fusion crust.

The slopes of the fractionation can give insights into the fractionation process (e.g., Young et al. 2002; Pack and Herwartz 2014), and theory predicts that the slopes can vary between 0.5 and 0.5305 for mass dependent isotope fractionation (Young et al. 2002). Slopes that exceed this limit are indicative of mass-independent processes, mixing, or coupling of different processes with different slopes and fractionations in $\delta^{18}O$. The slopes (defined by bulk meteorite—fusion crust pairs) from our study are within error identical to the upper limit for mass fractionation. The slopes for Allende (1.34) and Murchison (0.85), however, are significantly higher than the upper limit for mass fractionation of oxygen of 0.53 (Fig. 7B). Because both bulk samples and fusion crusts were analyzed in the same laboratory, an analytical artifact is unlikely. Such high slopes cannot be explained with a single mass fractionation trend. This suggests that the exchange between atmospheric O_2 and fusion crust is more complex than simple binary mixing or evaporation enrichments. If diffusion of O_2 is a controlling factor for the O isotope exchange, the $\delta^{18}O$ of the O_2 that is seen by the melt surface may be lower than that of ambient atmospheric O_2 and would explain the much steeper mixing trend observed for Murchison, but not Allende and the ordinary chondrite data (Fig. 7).

Alternatively, exchange of the melt with a high $\Delta^{17}O$ reservoir, such as stratospheric ozone ($\delta^{17}O \approx \delta^{18}O \approx 120‰$, $\Delta^{17}O \approx 60‰$; Thiemens 2006) may explain the observed difference between meteorite interior and fusion crust (Fig. 7). However, ozone concentrations in the stratosphere are in the ppm range only (Chance et al. 1997). For Murchison and Allende, only ~1% equilibration with stratospheric ozone explains the observed deviation from a simple mixing trend with atmospheric O_2. The concentration of ozone is <<1%, but its higher reactivity compared to O_2 may lead to faster exchange with the fused outer shell of meteorites at altitudes of ~20 km.

The small, if significant, deviation of the ordinary fusion crust data from a mixing trend require only about 0.1–0.2% equilibration with ozone. As ozone concentrations in the atmosphere are highest in the ozone layer, it may be speculated that the large deviations of Allende and Murchison from a mixing trend indicate that their fusion crust formed at an altitude of ~20 km where maximum ozone concentrations are established.

CONCLUSIONS

The Fe isotope signatures of fusion crusts from meteorite finds reflect two distinct contributions generated by (1) evaporation during atmospheric entry in a high-pressure environment, which produces fractionation in $\delta^{56}Fe$ of up to +0.30‰ and (2) terrestrial weathering, which fractionates $\delta^{56}Fe$ by up to about +0.1‰. Fusion crusts of meteorite falls only carry the evaporative signature. Chondrules have a comparatively small range of Fe isotope compositions ($\delta^{56}Fe$ from −1.33 to +0.65‰) that were established during evaporation and recondensation processes in the solar nebula. The similar extent of heavy Fe isotope enrichment in fusion crusts and chondrules supports the conclusion that chondrules formed in a high-pressure environment, which prevented large isotope fractionations.

The enrichments of $\delta^{18}O$ in at least some chondrite meteorite fusion crusts are partly due to minor O isotope exchange with Earth's atmosphere. Elevated $\Delta^{17}O$ values in fusion crust compared to the bulk meteorite are explained by mass transfer of isotopically anomalous stratospheric O_3 into the oxidation products of the fusion crust. Differences in the degree of exchange may reflect differences in altitude, whereby the higher degree of exchange inferred for Allende and Murchison may indicate formation of their fusion crust in the ozone layer. These observations furthermore support the interpretation that the variable, nonmass dependent O isotope compositions of chondrules were established by exchange of O between a chondrule melt and an ^{16}O-poor nebula (Yu et al. 1995; Chaussidon et al. 2008; Schrader et al. 2013, 2014).

Chondrule formation would be much easier to understand if we had a natural analogue. Here, we suggest that the formation of meteorite fusion crusts resembles, at least to some extent, chondrule formation. In fact, it may be the closest natural analogue available for chondrule formation. This conclusion is further supported by the similar Fe isotope fractionations observed for fusion crusts and chondrules. Differences in the extent of Fe isotope fractionations are the result of the different conditions that characterized the formation of fusion crusts and chondrules.

Acknowledgments—We thank the Paneth Trust for funding of this project. Deborah Cassey is thanked for her assistance in selecting meteorites. D. H. is indebted to Lukas Shrbeny for valuable discussions regarding the physical conditions during the atmospheric entry of meteorites. Kun Wang and Devin Schrader provided constructive reviews that helped to improve the initial submission and clarify critical points. We thank the AE Ian Franchi for his editorial work and comments that made this a better paper. Stanislav Strekopytov, Tony Wighton, John Spratt, and Lauren Howard provided invaluable assistance for the analytical work. D. H. dedicates this work to Katharina Stade for her support throughout the great British years.

Editorial Handling—Dr. Ian Franchi

REFERENCES

Alexander C. M. O'D., Taylor S., Delaney J. S., Peixue M. A., and Herzog G. F. 2002. Mass-dependent fractionation of Mg, Si, and Fe isotopes in five stony cosmic spherules. *Geochimica et Cosmochimica Acta* 66:173–183.

Alexander C. M. O'D., Grossman J. N., Ebel D. S., and Ciesla F. J. 2008. The formation conditions of chondrules and chondrites. *Science* 320:1617–1619.

Al-Kathiri A., Hofmann B. A., Jull A. J. T., and Gnos E. 2005. Weathering of meteorites from Oman: Correlation of chemical and mineralogical weathering proxies with ^{14}C terrestrial ages and the influence of soil chemistry. *Meteoritics & Planetary Science* 40:1215–1239.

Barkan E. and Luz B. 2011. The relationships among the three stable isotopes of oxygen in air, seawater and marine photosynthesis. *Rapid Communications in Mass Spectrometry* 25:2367–2369.

Chance K. V., Burrows J. P., Perner B. D., and Schneider W. 1997. Satellite measurements of atmospheric ozone profiles, including tropospheric ozone, from ultraviolet/visible measurements in the nadir geometry: A potential method to retrieve tropospheric ozone. *Journal of Quantitative Spectroscopy and Radiative Transfer* 57:467–476.

Chaussidon M., Libourel G., and Krot A. N. 2008. Oxygen isotopic constraints on the origin of magnesian chondrules and on the gaseous reservoirs in the early solar system. *Geochimica et Cosmochimica Acta* 72:1924–1938.

Chladni E. F. F. 1819. *Über Feuer-Meteore und die mit denselben herabgefallenen Massen*. Vienna: J.G. Heubner. 434 p.

Choi B.-G., Nakamura T., and Kusakabe M. 2007. Ion microprobe measurements of oxygen isotope compositions of artificial chondrules and CAI: Implications for nebular oxygen exchange during the formation of chondrules and CAIs (abstract #1054). 38th Lunar and Planetary Science Conference. CD-ROM.

Clayton R. N., Mayeda T. K., Hutcheon I. D., Molini-Velsko C., Onuma N., Ikeda Y., and Olsen E. J. 1983. Oxygen isotopic compositions of chondrules in Allende and ordinary chondrites. In *Chondrules and their origins*, edited by King E. A. Houston, Texas: Lunar and Planetary Institute. pp. 37–43.

Clayton R. N., Mayeda T. K., and Brownlee D. E. 1986. Oxygen isotopes in deep-sea spherules. *Earth and Planetary Science Letters* 79:235–240.

Craddock P. R. and Dauphas N. 2011. Iron isotopic compositions of geological reference materials and chondrites. *Geostandards and Geoanalytical Research* 35:101–112.

Cuzzi J. N. and Alexander C. M. O'D. 2006. Chondrule formation in particle-rich nebular regions at least hundreds of kilometres across. *Nature* 441:483–485.

Dauphas N., Janney P. E., Mendybaev R. A., Wadhwa M., Richter F. M., Davis A. M., van Zuilen M., Hines R., and Foley C. N. 2004. Chromatographic separation and multicollection-ICPMS analysis of iron. Investigating mass-dependent and -independent isotope effects. *Analytical Chemistry* 76:5855–5863.

Engrand C., McKeegan K. D., Leshin L. A., Herzog G. F., Schnabel C., Nyquist L. E., and Brownlee D. E. 2005. Isotopic compositions of oxygen, iron, chromium, and nickel in cosmic spherules: Toward a better comprehension of atmospheric entry heating effects. *Geochimica et Cosmochimica Acta* 69:21–28.

Genge M. and Grady M. 1999. The fusion crusts of stony meteorites: Implications for the atmospheric reprocessing of extraterrestrial materials. *Meteoritics & Planetary Science* 34:341–356.

Hezel D. C. and Palme H. 2007. The conditions of chondrule formation, Part I: Closed system. *Geochimica et Cosmochimica Acta* 71:4092–4107.

Hezel D. C., Needham A. W., Armytage R., Georg B., Abel R. L., Kurahashi E., Coles B. J., Rehkaemper M., and Russell S. S. 2010. A nebula setting as the origin for bulk chondrule Fe isotope variations in CV chondrites. *Earth and Planetary Science Letters* 296:423–433.

Hezel D. C., Schlüter J., Kallweit H., Jull A. J. T., Al Fakeer O. Y., Al Shamsi M., and Strekopytov S. 2011. Meteorites from the United Arab Emirates: Description, weathering, and terrestrial ages. *Meteoritics & Planetary Science* 46:327–336.

Humayun M. and Clayton R. N. 1995. Potassium isotope cosmochemistry: Genetic implications of volatile element depletion. *Geochimica et Cosmochimica Acta* 59:2131–2148.

Jull A. J. T. 2006. Terrestrial ages of meteorites. In *Meteorites in the early solar system II*, edited by Lauretta D. and McSween H. Y. Jr. Tucson, Arizona: The University of Arizona Press. pp. 889–905.

Kroopnick P. and Craig H. 1972. Atmospheric oxygen: Isotopic composition and solubility fractionation. *Science* 175:54–55.

Krot A. N., Yurimoto H., McKeegan K. D., Leshin L., Chaussidon M., Libourel G., Yoshitake M., Huss G. R., Guan Y., and Zanda B. 2006. Oxygen isotopic compositions of chondrules: Implications for evolution of oxygen isotopic reservoirs in the inner solar nebula. *Chemie der Erde—Geochemistry*, 66:249–276.

Lodders K. and Fegley B. 1998. *The planetary scientist's companion*. New York: Oxford University Press.

Miller M. F. 2002. Isotopic fractionation and the quantification of ^{17}O anomalies in the oxygen three-isotope system: An appraisal and geochemical significance. *Geochimica et Cosmochimica Acta* 39:569–584.

Molini-Velsko C., Mayeda T. K., and Clayton R. N. 1986. Isotopic composition of silicon in meteorites. *Geochimica et Cosmochimica Acta* 50:2719–2726.

Mullane E., Russell S., and Gounelle M. 2005. Nebular and asteroidal modification of the iron isotope composition of chondritic components. *Earth and Planetary Science Letters* 239:203–218.

Needham A. W., Porcelli D., and Russell S. S. 2009. An Fe isotope study of ordinary chondrites. *Geochimica et Cosmochimica Acta* 73:7399–7413.

Pack A. and Herwartz D. 2014. The triple oxygen isotope composition of the Earth mantle and $\Delta^{17}O$ variations in terrestrial rocks. *Earth and Planetary Science Letters* 390:138–145.

Pack A., Yurimoto H., and Palme H. 2004. Petrographic and oxygen-isotope study of refractory forsterites from R-chondrite Dar al Gani 013 (R3.5-6), unequilibrated ordinary and carbonaceous chondrites. *Geochimica et Cosmochimica Acta* 39:569–584.

Pack A., Gehler A., and Süssenberger A. 2013. Exploring the usability of isotopically anomalous oxygen in bones and teeth as paleo-CO_2-barometer. *Geochimica et Cosmochimica Acta* 102:306–317.

Pouchou J. and Pichoir F. 1991. Quantitative analysis of homogeneous or stratified microvolumes applying the model "PAP". In *Electron probe quantification*, edited by Heinrich K. F. J. and Newbury D. E. New York: Plenum. pp. 31–75.

Ramdohr P. 1967. Die Schmelzkruste der Meteoriten. *Earth and Planetary Science Letters* 2:197–209.

Rudraswami N., Ushikubo T., Nakashima D., and Kita N. 2011. Oxygen isotope systematics of chondrules in the Allende CV3 chondrite: High precision ion microprobe studies. *Geochimica et Cosmochimica Acta* 75:7596–7611.

Saunier G., Poitrasson F., Moine B., Gregoire M., and Seddiki A. 2010. Effect of hot desert weathering on the bulk-rock iron isotope composition of L6 and H5 ordinary chondrites. *Meteoritics & Planetary Science* 45:195–209.

Schrader D. L., Connolly H. C. Jr., Lauretta D. S., Nagashima K., Huss G. R., Davidson J., and Domanik K. J. 2013. The formation and alteration of the Renazzo-like carbonaceous chondrites II: Linking O-isotope composition and oxidation state of chondrule olivine. *Geochimica et Cosmochimica Acta* 101:302–327.

Schrader D. L., Nagashima K., Krot A. N., Ogliore R. C., and Hellebrand E. 2014. Variations in the O-isotope composition of gas during the formation of chondrules from the CR chondrites. *Geochimica et Cosmochimica Acta* 132:50–74.

Sharp Z. D. 1990. A laser-based microanalytical technique for in situ determination of oxygen isotope ratios of silicates and oxides. *Geochimica et Cosmochimica Acta* 54:1353–1357.

Taylor S., Alexander C. M. O'D., Delaney J., Ma P., Herzog G. F., and Engrand C. 2005. Isotopic fractionation of iron, potassium, and oxygen in stony cosmic spherules: Implications for heating histories and sources. *Geochimica et Cosmochimica Acta* 69:2647–2662.

Thaisen K. G. and Taylor L. A. 2009. Meteorite fusion crust variability. *Meteoritics & Planetary Science* 44:871–878.

Thiemens M. H. 2006. History and applications of mass-independent isotope effects. *Annual Reviews in Earth Planetary Science Letters* 34:217–262.

Wang K., Moynier F., Barrat J.-A., Zanda B., Paniello R. C., and Savage P. S. 2013. Homogeneous distribution of Fe isotopes in the early solar nebula. *Meteoritics & Planetary Science* 48:354–364.

Young E. D., Galy A., and Nagahara H. 2002. Kinetic and equilibrium mass-dependent isotope fractionation laws in nature and their geochemical and cosmochemical significance. *Geochimica et Cosmochimica Acta* 66:1095–1104.

Yu Y., Hewins R. H., Clayton R. N., and Mayega T. K. 1995. Experimental study of high temperature oxygen isotope exchange during chondrule formation. *Geochimica et Cosmochimica Acta* 59:2095–2104.

Zhu X. K., Guo Y., O'Nions R. K., Young E. D., and Ash R. D. 2001. Isotopic homogeneity of iron in the early solar nebula. *Nature* 412:311–313.